IEEE Access
Multidisciplinary | Rapid Review | Open Access Journal

Date of publication xxxx 00, 0000, date of current version xxxx 00, 0000.

Digital Object Identifier 10.1109/ACCESS.2022.Doi Number

An Assessment of Shortest Prioritized Path Based Bidirectional Wireless Charging Approach Toward Smart Agriculture

Prithvi Krishna Chittoor[1], Bharatiraja Chokkalingam[1], (Senior Member, IEEE), Rajesh Verma[2], Lucian Mihet-Popa[3], (Senior Member, IEEE),

[1]Department of Electrical and Electronics Engineering, SRM Institute of Science and Technology, Kattankulathur, Tamil Nadu 603203, India
[2]Electrical Engineering Department, College of Engineering, King Khalid University, Abha, 61411, Asir, Kingdom of Saudi Arabia
[3]Faculty of Engineering, Østfold University College, 1757 Halden, Norway.

Corresponding author: Bharatiraja Chokkalingam (e-mail: bharatic@srmist.edu.in), Lucian Mihet-Popa (e-mail: lucian.mihet@hiof.no)

This research work is supported by the Department of Science and Technology, Government of India, Promotion of University Research and Scientific Excellence (PURSE), under Award SR/PURSE/2021/65 and Science and Engineering Research Board Core Research Grant (SERB CRG/2019/005483).

ABSTRACT The agriculture sector has witnessed a transformation with the advent of smart sensing devices, leading to improved crop yield and quality. However, the management of data collection from numerous sensors across vast agricultural areas, as well as the associated charging requirements, presents significant challenges. This paper addresses the major research problem by proposing an innovative solution for charging agricultural sensors. The introduction of an energy-constrained device (ECD) enables wireless charging and transmission of soil data to a centralized server. The proposed ECDs will enable enhanced data collection, precision agriculture, optimized resource allocation, timely decision-making, and remote monitoring and control. A bidirectional wireless charging drone is employed to efficiently charge the ECDs. To optimize energy usage, a prioritized Dijkstra algorithm determines the ECDs to be charged and plans the shortest route for the drone. The wireless charging drone landing-charging station achieves an efficiency of 91.3%, delivering 72 W of power within a 5 mm range. Furthermore, the ECD possesses a data transmission range of 100 m and incorporates deep sleep functionality, allowing for a remarkable 30-day battery life.

INDEX TERMS Bidirectional charging, Dijkstra, Inductive Power Transfer, UAV, Wireless Charging.

I. INTRODUCTION

Agriculture has always been a labor-intensive profession, needing constant care for the crops and monitoring. Due to the variety of landforms, drones are ideal machinery for the autonomous monitoring of crops, as they work independently of landscape and terrain [1, 2]. The current commercial lightweight drone market is focusing on photography, sample collection, disaster management, transport delivery, and, recently, pesticide spraying in the agricultural fields [3-6]. However, drones alone cannot accurately determine the needs of the crops; thus, the concept of sensor-based Energy Constrained Devices (ECDs) is introduced in this paper. ECDs are small, fully enclosed, waterproof sensory devices that gather the soil parameters and periodically send the collected data to the central server via radio frequency (RF) signals. An array of these devices help in understanding the immediate need of a particular area and aids in generating a long-term profile of that particular region. Since the soil sensor ECDs are planted in the ground and are fully enclosed, it is difficult to replace their battery frequently, thus the concept of a wireless charging method is introduced.

Previous studies on similar technologies have shown the interest of researchers moving toward the automation of the agricultural field. Sadowski *et al.* developed a smart agricultural monitoring Internet of Things (IoT) device powered by a 6600 mAh Lithium Polymer (LiPo) battery that monitors soil moisture. The author's comparison study indicated that compared to WiFi, RF-based communication has significantly less power consumption and transmits over a wide distance [7]. Similarly, Sharma *et al.* proposed to maximize the device's lifetime by reducing its operation's duty cycle to 25%. This increased the device's lifetime from 5.75 days to 115.75 days. Although the system has a lifetime of 115 days, the non-rechargeable batteries make the device semi-automated, requiring human intervention [8].

Sambo *et al.* tackle the signal attenuation problem of wireless signals penetrating the underground using a low-

powered near-RF (nRF) signal transceiver of 433 MHz. The author developed a path loss model for precision agriculture where the devices are embedded into the ground and transmit soil prediction parameters to a transceiver. The author claimed to achieve 87.13% precision and 85% balanced accuracy. However, the problem of charging these devices persists [9]. Similar research on improving node routing was discussed in [10] and [11], where the authors used clustering algorithms and positioning algorithms. The author proposed simulation models to show the simulated energy consumption model and reduced positioning errors. Furthermore, a simple tree-like communication model was proposed to gather data from individual nodes.

For drone path planning, Jun *et al.* [12] proposed an ant colony and A* hybrid algorithm for battery exchange and maintenance for long-range drone travel and path planning. The algorithm shows promising results when traveling in a sequential path over large distances. The Euclidean shortest path method is solved by using the hybrid ant colony and A* method.

Rashid *et al.* [13] proposed the of use a traveling salesman algorithm for path planning and discussed the power consumption model of the drone during travel. The drone is able to charge itself wirelessly with the help of a robotic arm fitted with an inductive charging pad. Similar approaches were made by [14, 15] using the traveling salesman problem for identifying drone charging stations. However, the traveling salesman problem gives a large number of possible routes for the drone to travel and does not take into consideration the priority set by each node.

Pericle *et al.* [16] proposed a sequential path-planning algorithm for localizing nodes in a given area using a combination of three algorithms: LocalizerBee, VerifierBee, and PreciseVerifierBee. The nodes are placed in a regular interval pattern for the drone to identify the position.

Rosello *et al.* [17] proposed an information-driven path-planning algorithm for Unmanned Aeriel Vehicles (UAVs) using a boustrophedon pattern for covering a large field, however, the algorithm does not take into consideration the priority of nodes.

In the past decade, drone-based agricultural applications have seen a rise due to the ease of maneuverability in tight spaces and their autonomous capabilities. Jawad *et al.* proposed a wireless charging drone with a sleep/active strategy to conserve power. The author demonstrated a 20.46 W, 85.25% efficient photovoltaic (PV) powered wireless power transmission (WPT) system to charge a drone [18].

Su *et al.* proposed a wireless charging ECD system using a dynamic matching technique via an UAV. The author demonstrated a simulated case study of the charging system and investigated the energy consumption of ECDs [19]. Although the author proposed the wireless charging ECD concept, a detailed study on the hardware implementation is lacking and requires attention.

The concept of bidirectional wireless charging is not new from the available literature, the studies have mainly concentrated on electric car charging or bulky system [20-22],[30]-[34]. Wang *et al.* proposed a 200 kHz bidirectional wireless system that can charge up to 5 mm coil spacing distance to a maximum of 7.8 W [23].

Li *et al.* proposed a 41.2 W drone wireless charging system and a 15.8 W sensor charging system, however, a significant amount of time was consumed for charging [24]. Thus, a fast-charging WPT system needs to be studied. The literature of previous studies indicates that experimental studies on battery charging techniques of underground ECDs are lacking, a prioritized path planning system has not been proposed for wireless ECD charging in agricultural applications, bidirectional wireless charging UAV system needs to be experimentally studied.

The proposed system is illustrated in Fig. 1. The charging pad consists of a PV-powered high-frequency charging circuit and the transmitter (Tx) coil. The drone consists of a WPT coil which acts as both Tx and receiver (Rx) coil, and the internal WPT circuit to charge the drone's battery. The ECD consists of a rectification circuit, controller, and sensors for retrieving environmental parameters. The contributions of the study can be summarized as follows:

a. Development of 72 W, 91.3% efficient wireless drone charging station, bidirectional wireless charging drone, and a wireless charging ECD with 30 days battery life.
b. Study of shortest path charging strategy for a 5 W, 5- 10 mm wireless charging ECD sensors using prioritized Dijkstra's algorithm.
c. The proposed ECDs will enable enhanced data collection, precision agriculture, optimized resource allocation, timely decision-making, and remote monitoring and control.
d. Experimental evaluation of wireless power transfer efficiency.
e. Theoretical analysis and case studies of proposed Dijkstra's algorithm compared with conventional path planning method.

II. PROPOSED SYSTEM ARCHITECTURE

The proposed system is divided into three parts: wireless drone landing-charging station, wireless bidirectional charging drone, and wireless charging ECD.

A. DRONE LANDING-CHARGING STATION

The drone landing-charging station consists of major elements such as the PV panel, maximum power point tracking (MPPT), H-Bridge MOSFET inverter, Series-Series compensation network and the Tx coil made of Litz material, illustrated in Fig. 1. Furthermore, the setup consists of a Spartan 6 FPGA microcontroller that triggers the custom made MOSFET drivers using IRF9530 and IRF530 switches (named S_1, S_2, S_3, and S_4), 130 W PV panel, and a 300 W SolarEdge power optimizer. The server is responsible for initiating the power transfer when the drone lands at the landing station.

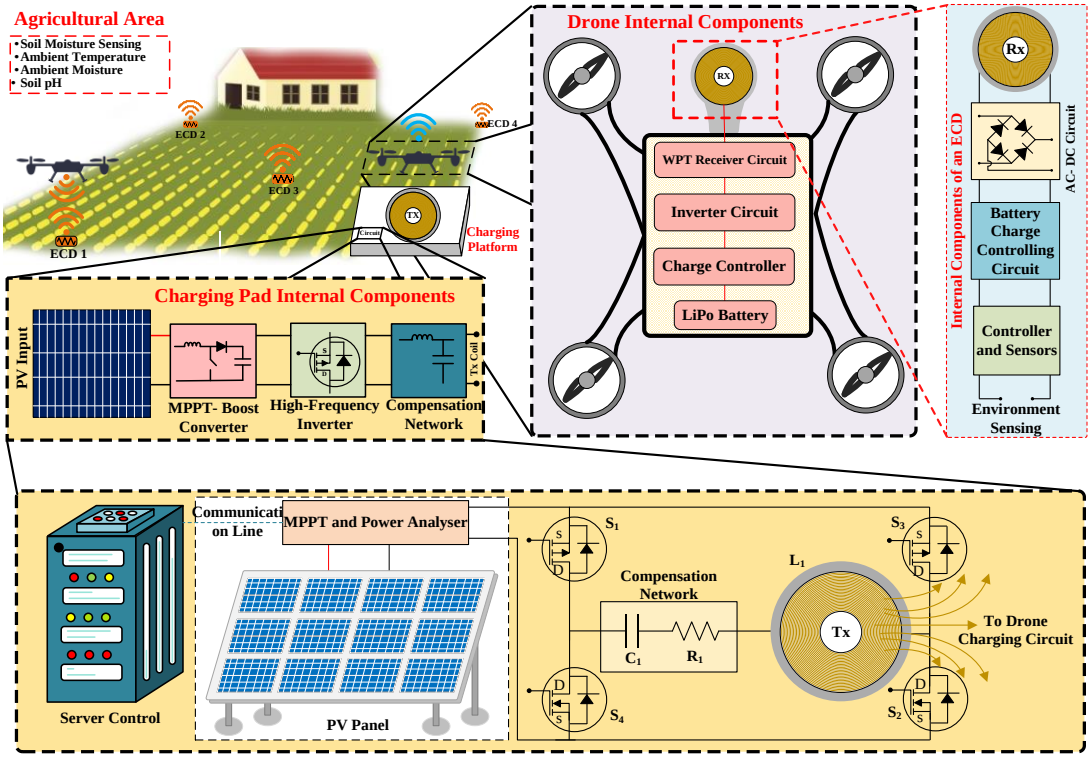

FIGURE 1. **Proposed Wireless Soil Node Charging System**

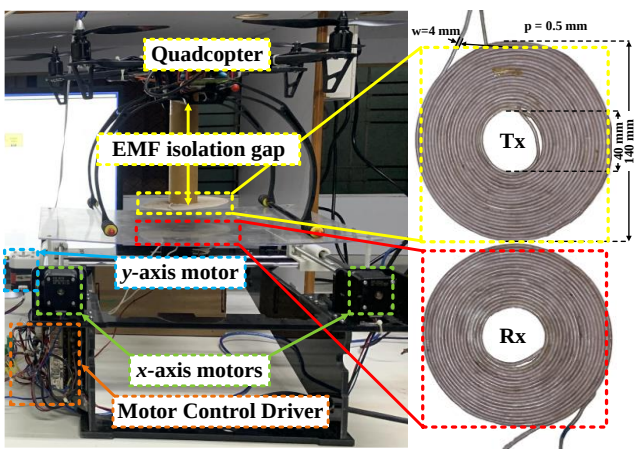

FIGURE 2. **Wireless Drone Charging Experimental Setup with EMF Isolation Gap**

Fig. 2 shows the identical Tx-Rx coils used for the experiment and the landing station. Previous studies have shown that the maximum efficiency of WPT for circular coils can be achieved in the range of 60 – 270 kHz of operation [25-28]. An 84 kHz and 50% duty cycle pulse signal are applied to the MOSFETs during the charging cycle. A 20 cm gap between the Rx coil and the drone's internal circuit is provided to prevent the Tx-Rx coil's Electromotive force (EMF) from interacting with the drone's charging circuit. A detailed summary of the components used in developing the drone landing-charging station is presented in Table I.

B. BIDIRECTIONAL WIRELESS CHARGING DRONE

Literature studies [26, 29-31] has indicated that the Ansys Maxwell EMF simulation tool helps in modeling the EMF transmission between Tx and Rx coils. Additionally, it has been shown to be effective in determining the location of the region where the maximum EMF is generated. The simulation software can identify any potential areas of weakness in the coil design and inefficiencies in the system.

Fig. 3, and Table II illustrate the EMF heat map for various lateral displacements of the proposed coil structure, which consists of 20 turns, 2 mm width, 0.1 mm pitch, and 58.6 µH inductance.

For a circular WPT coil when the coils are aligned perfectly on top of each other, the maximum EMF is generated at the centre of the coils. If the centre of the coil is not perfectly aligned, a significant drop in the coupling coefficient is observed, leading to a drop in power.

Fig. 4(a) and 4(b) depicts the effect of WPT's EMF on the proposed agriculture drone and on a regular bird of 150 mm height; it shows that the flux transfer distance is not more than 50 mm, thus having very minute effect on the bird.

TABLE I. Specifications of Landing Station, ECD and Drone Components

Parameter	Model and Specifications	Parameter	Specifications
Landing Station Parameters		**ECD Internal Components**	
Inductance (L)	Circular 15.19µH	Microcontroller	ESP8266, 3.3 V, 170 mA, 15µA during deep sleep
Capacitance (C)	231 nF	nrf24l01 RF-Transmitter	13 mA during receiving, 11 mA during transmission, 22 µA during standby, minimum 250 Kbps transfer rate, range 100 m
Number of Turns (N)	20	LiPo battery	4.2 V, 600 mAh, 25 C discharge
Outer Diameter of coil (D_{out})	160 mm	LiPo Charger	TP4056, 4.5-5.2V, 1~1.2A charge current handling capacity
Pitch of coil (*p*)	0.5 mm	Soil Moisture sensor	Grove soil moisture sensor, 3.3-5 V operating voltage, operating current < 20 mA
Width of Conductor (w)	4 mm	Wireless coil system	5 V, 1.2 A
Frequency (*f*)	84 kHz	**Drone Parameters**	
Quality Factor (Q)	169	LiPo Battery, 11.1 V, 3000 mAh, 40 C	141 g
MOSFET	IRF9530 and IRF530	Tx/Rx coil, 20 turns, 4 mm width, 0.5 mm pitch	125 g
Microcontroller	Spartan 6 FPGA	Charge controller	110 g
Stepper motor	Hybrid 2 Phase, 42 steps, 1.8º	Carbon fiber chassis	400 g
Motor Driver	DRV8825 stepper motor driver	Motors, ESCs, flight controller	500 g
Tx/Rx coil weight	125 grams each	Landing gear	230 g
PV Panel	26 V, 6 A	Accessories- camera, GPS, nuts, switches, propellers	180 g
Power Optimizer	SolarEdge 300 W	**Total UAV Weight**	**1.68 kg**

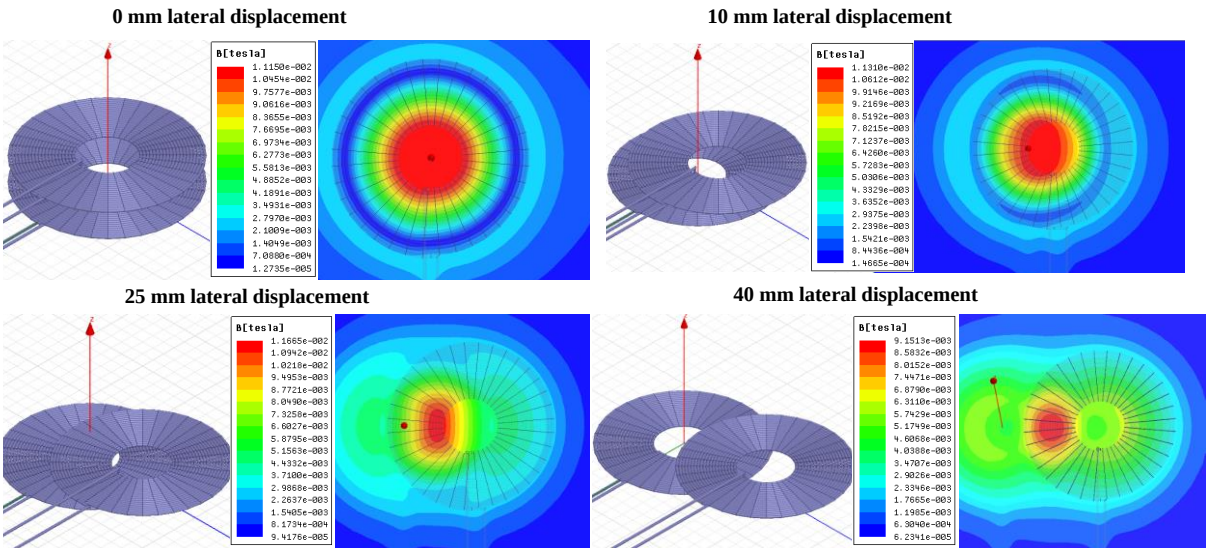

FIGURE 3. EMF Heat Map for Various Lateral Displacements

TABLE II. EMF vs. lateral displacement between coils

Distance between coils (mm)	0	10	25	40
B ($\times 10^{-2}$ Tesla)	1.1150	1.1310	1.1665	0.9151

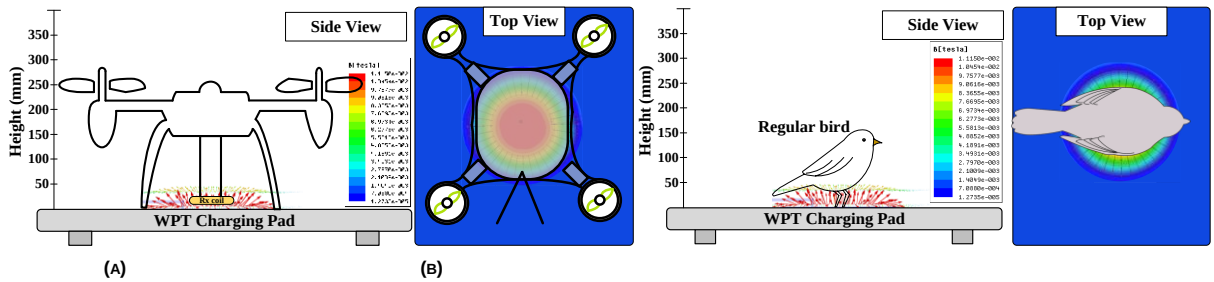

FIGURE 4. Effect of EMF on (a) agriculture drone (b) Regular bird

C. MODELLING OF A BIDIRECTIONAL CHARGING CIRCUIT

In a bidirectional charging circuit, the transmitter and the receiver side inverter circuit are identical. For a full bridge CLLC type converter, shown in Fig. 5, L_T is the transmitter side resonant inductor, L_R is the receiver side resonant inductor, C_T is the transmitter side resonant capacitor, C_R is the receiver side resonant capacitor, L_m be the magnetising inductance and the turns ratio be n:1. In charging mode (Fig. 6(a), let R_e be the equivalent of R_o, L'_R be the equivalent of L_R, C'_R be the equivalent of C_R, represented in the transmitter side. The transfer function of the proposed CLLC converter is determined by Eq. (1).

$$H(s) = \frac{1}{n} \cdot \frac{R_e}{R_e + Z'_{LR} + Z'_{CR}} \cdot \frac{(R_e + Z'_{LR} + Z'_{CR}) || Z_{Lm}}{Z_{LT} + Z_{CT} + (R_e + Z'_{LR} + Z'_{CR}) || Z_{Lm}} \quad (1)$$

Thus, the gain of the full bridge CLLC converter is calculated by using Eq. (2).

$$G_{CLLC} = |H(s)| = \left|\frac{V_{out}}{V_{in}}\right| = \frac{1}{n} \cdot \frac{1}{\sqrt{a^2 + b^2}} \quad (2)$$

Where,

$$a = \frac{1}{h} + 1 - \frac{1}{h \cdot \omega^2},$$

$$b = \left(\frac{k}{h} + 1 + \frac{1}{g \cdot h} + \frac{1}{g}\right) \frac{Q}{\omega} - \left(\frac{k}{h} + 1 + k\right) Q \cdot \omega - \frac{Q}{g \cdot h \cdot \omega^3},$$

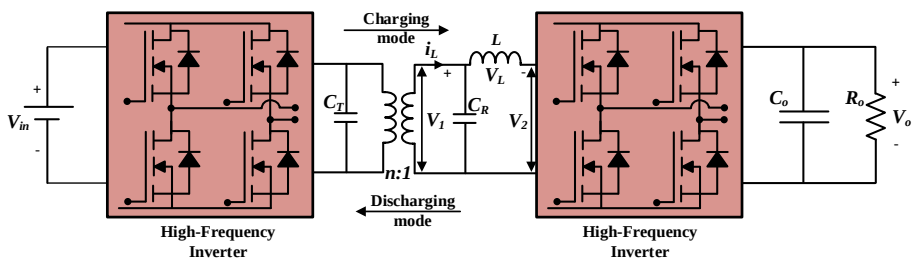

FIGURE 5. Bidirectional full bridge resonant converter

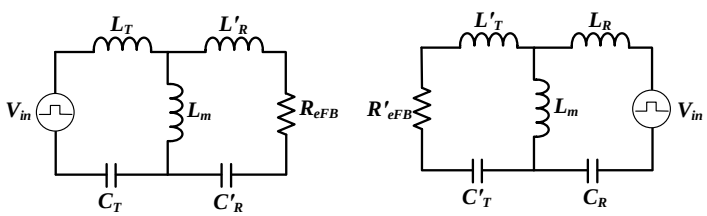

FIGURE 6. Equivalent circuit of a full bridge resonant converter during (a) charging and (b) discharging mode

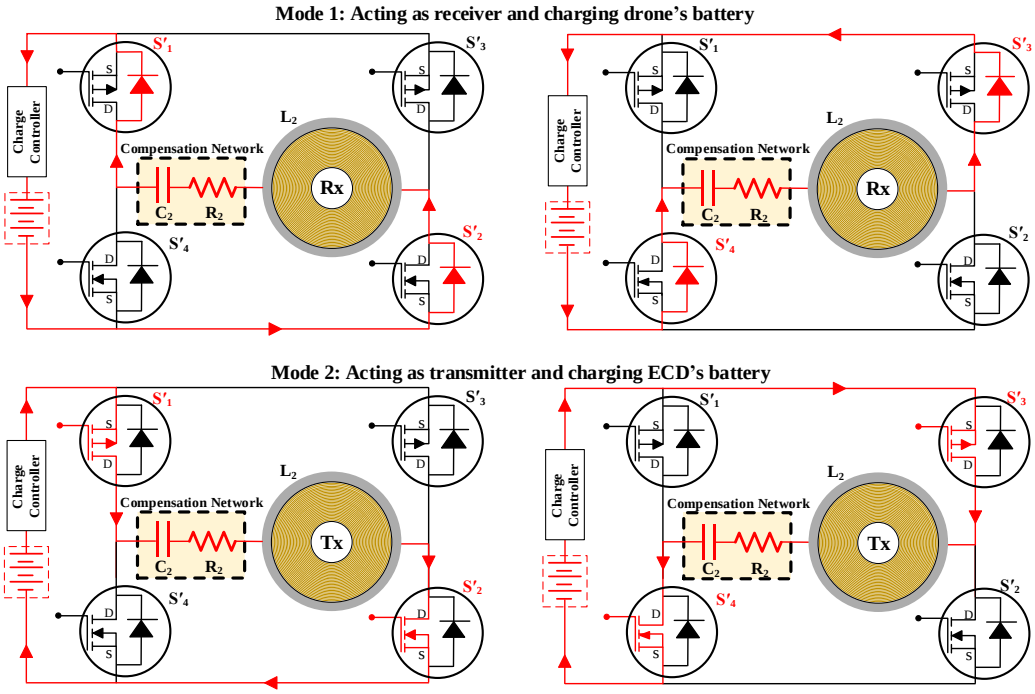

FIGURE 7. Mode 1 (Drone battery charging from landing station) and Mode 2 (ECD battery charging from drone battery) of Wireless Bidirectional Drone Charging

$$h = \frac{L_m}{L_T}, k = \frac{L'_R}{L_T}, g = \frac{C'_R}{C_T}, \omega = \frac{\omega_s}{\omega_r},$$
$$\omega_r = \frac{1}{\sqrt{L_T C_T}}, Q = \frac{\sqrt{L_T/C_T}}{R_e}$$

Here, ω_r represents the resonant frequency, ω_s represents the operating frequency, ω represents the normalized frequency and Q is the quality factor. To calculate the equivalent load in the charging circuit, first harmonic approximation is used. For the proposed full bridge CLLC converter, the equivalent load, inductance and capacitance is given by Eq. (3).

$$R_{e,FB} = \left(\frac{8n^2}{\pi^2}\right) R_o, L'_R = n^2 L_R, C'_R = \frac{C_R}{n^2} \quad (3)$$

Fig. 6(b) represents the discharging mode equivalent circuit of the full bridge CLLC converter. The equivalent load, inductance and capacitance is given by Eq. (4).

$$R'_{e,FB} = \left(\frac{8}{n^2\pi^2}\right) R'_o, L'_T = \frac{L_R}{n^2}, C'_T = n^2 C_R, \text{and } L_m = \frac{L_m}{n^2} \quad (4)$$

The gain of the full bridge CLLC converter during discharging mode is defined by Eq. (5).

$$G_{CLLC} = n \cdot \frac{1}{\sqrt{c^2 + d^2}} \quad (5)$$

Where, $c = \frac{1}{h'} + 1 - \frac{1}{h' \cdot \omega'^2}$,

$$d = \left(\frac{k'}{h'} + 1 + \frac{1}{g' \cdot h'} + \frac{1}{g'}\right)\frac{Q'}{\omega'} - \left(\frac{k'}{h'} + 1 + k'\right) Q'\omega' - \frac{Q'}{g' \cdot h' \cdot \omega'^3}$$

Here, L and C maintains their previous value, ω'_r, k', g', and h' maintains the equivalent value of ω_r, k, g, and h, respectively as in the charging mode. Since, the equivalent load has change in the discharging mode, the Q' is calculated by Eq. (6).

$$Q' = \frac{n^2 R_o}{R'_o Q} \quad (6)$$

The proposed bidirectional wireless charging/discharging drone is equipped with a 3000 mAh, 40 C discharge rate, three-cell battery is connected to a balance charger controller and H-Bridge inverter circuit, as shown in Fig. 7. The weight distribution of the UAV is presented in Table I. The charge controller help in two major functions of the bidirectional wireless charging/discharging drone: maintaining the balance charge condition between the cells of the battery and acting as a controller for charging/discharging condition.

Fig. 7 represent the two modes of operation of the drone's WPT circuit. In the first mode of operation, shown in Fig. 7 Mode 1, the WPT coil acts as the Rx. During the positive half cycle of the Rx waveform, the antiparallel diodes of the MOSFETs S'_1 and S'_2 pass it to the charge controller and during the negative phase of the Rx signal, S'_3 and S'_4 pass the signal. In the second mode of operation, the MOSFETs are triggered to generate high-frequency AC signals. During this condition, the WPT coil acts as the Tx coil, supplying EMF to the ECD's Rx coil. The flow of energy from the battery to the Tx coil can be seen in Fig. 7 Mode 2. This kind of MOSFET arrangement reduces the need for an external rectification circuit, further reducing the weight of the drone.

D. WIRELESS CHARGING ECD

The concept of wireless charging in the ECD is introduced since the sensor module will be buried underground and to charge the internal battery, it has to be dug up. Instead, wireless charging of the ECD using an automated

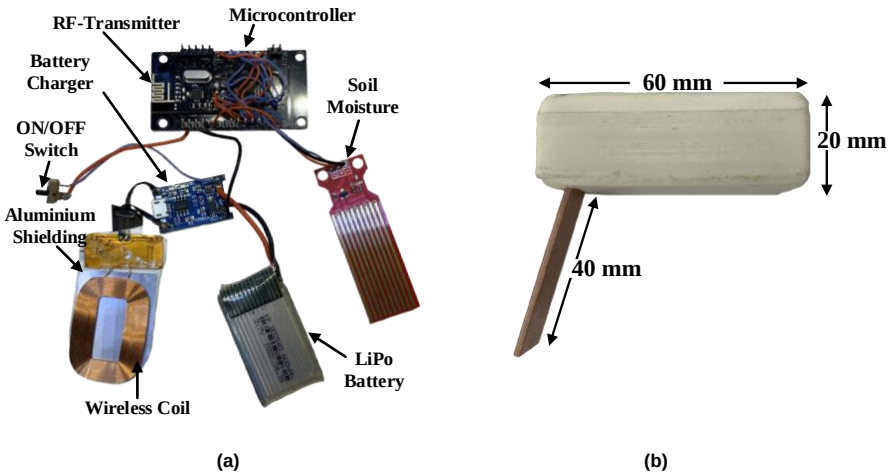

FIGURE 8. **(a) ECD's Internal Components (b) ECD Packed Module**

drone will provide complete autonomous charging infrastructure to the agricultural sensing architecture.

1) Design of ECD

The proposed ECDs is a compact microcontroller-sensor setup with an in-built rechargeable LiPo battery, 5V battery charger, RF transmitter, soil moisture sensors and a 5V Rx receiver-rectification circuit. The internal components of the ECD module is shown in Fig. 8 (a). The packed system setup of the ECD is shown in Fig. 8 (b). When the drone's WPT system is acting in Mode 2, it is crucial to protect the internal components from the EMF of the drone's Tx coil. Thus, a thin aluminium shielding is provided beneath the ECD's Rx coil. This shielding prevents the drone's Tx coil from affecting the internal components of the ECD. The internal components used in the development of the ECD are shown in Table I.

2) ECD's Power Consumption Model

It is essential to understand how long the battery would last before it requires further recharging. Thus, the following equations estimate the power consumption and the frequency at which each ECD needs to be charged. The total battery life of an ECD can be given by Eq. (7).

$$Battery\ Life = \frac{Battery\ Capacity}{Average\ Consumption} \times (1 - Discharge\ Safety) \quad (7)$$

Where battery life is the amount of time in hours the battery would work before getting completely discharged, battery capacity is the rating of the battery in mAh, average consumption is the current consumed during its working cycle in mAh and discharge safety is the minimum limit set before the battery requires recharging (consider it to be 20%).

For the proposed system, let I_{Total} be the total current consumed by the ECD, which is divided into two parts: when it is working (I_{Awake}) and when it is in a deep sleep (I_{Sleep}). During its data transmission, the current is consumed by the microcontroller (denoted as $I_{MCawake}$), RF-transmitter ($I_{RFawake}$) and soil sensor ($I_{Soilawake}$). Similarly, the current consumed during deep sleep is denoted as $I_{MCsleep}$, $I_{RFsleep}$ and $I_{Soilsleep}$ for the microcontroller, RF-transmitter and soil sensor, respectively. Some losses during power conversion and data transmission is denoted as I_{Loss}. T_{ON1} is the initial time when the system turns ON from deep sleep to measure and transfer data, T_{OFF1} is when the system switches back to a deep sleep state, and T_{ON2} is the time of the next data recording cycle. Then, Average consumption is given by (8)-(11).

$$I_{Total} = \int_{T_{ON1}}^{T_{OFF1}} \left(I_{Awake}(t) \times \int_{T_{ON1}}^{T_{OFF1}} t\right) + \int_{T_{OFF1}}^{T_{ON2}} \left(I_{Sleep}(t) \times \int_{T_{OFF1}}^{T_{ON2}} t\right) + I_{Loss} \quad (8)$$

$$\mathrm{I_{Awake}} = \mathrm{I_{MCawake}} + \mathrm{I_{RFawake}} + \mathrm{I_{Soilawake}} \quad (9)$$

$$\mathrm{I_{Sleep}} = \mathrm{I_{MCsleep}} + \mathrm{I_{RFsleep}} + \mathrm{I_{Soilsleep}} \quad (10)$$

$$\text{Average Consumption} = \frac{\mathrm{I_{Total}}}{\int_{T_{ON1}}^{T_{OFF1}} t + \int_{T_{OFF1}}^{T_{ON2}} t} \quad (11)$$

For the proposed 600 mAh battery, I_{Awake} is 220 mAh, I_{Sleep} is 37 µAh and I_{Loss} is taken as 30 mAh. Considering the system runs for 10 seconds and sleeps for 50 seconds, the Average Consumption becomes 37.20 mAh; thus, the battery life is approximately 12 hours and 54 minutes (Table III). The battery is operated for 80% of its full charge capacity, i.e. 80% of 600 mAh, which is 480 mAh. Thus, the percentage decrease

TABLE III. **Battery Lifetime Estimations of ECD**

Usage Duration	Battery Lifetime	
	Hours	Days
10 seconds per minute	12 hours 54 minutes	0.54 days
10 seconds per 5 minutes	64 hours 15 minutes	2.68 days
10 seconds per 10 minutes	127 hours 53 minutes	5.33 days
10 seconds per 15 minutes	190 hours 54 minutes	7.95 days
10 seconds per 30 minutes	376 hours 27 minutes	15.68 days
10 seconds per 1 hour	731 hours 33 minutes	30.47 days
10 seconds per 2 hours	1384 hours 35 minutes	57.69 days

per cycle of operation (L_{Cycle}) is given by, 100%/13 hour = approximately 7.7% decrease per hour. This can be further increased by increasing the deep sleep duration, as a soil sensor doesn't need such a fast data transmission time.

3) ECD's Charging Time Model

The time required for charging individual ECD can be determined by the approximated time consumption model based on Eq. (12). It determines that the Nth ECD's charging time is the total sum of the time required to travel and charge the previous ECDs. The travel time is further divided into the takeoff time, distance travel time and landing time, Eq.(13). Thus, time taken to charge is:

$$T_{N^{th}Total} = \sum_{i=1}^{N-1}(T_{i_{Travel}} + T_{i_{Charge}}) + T^*_{N^{th}Charge} \quad (12)$$

$$T_{i_{Travel}} = T_{iTakeoff} + T_{\text{iDistance}} + T_{iLand} \quad (13)$$

$$T^*_{N^{th}Charge} = (SoC_{Maximum} - T_{NCurrent}) \times CC \quad (14)$$

Similarly, $T_{iCharge} = (SoC_{Maximum} - T_{NCurrent}) \times CC$ (15)

Where $T_{N^{th}Total}$ is the total time required to charge the N^{th} ECD, $T_{iTravel}$ is the time required to travel from (i-1) node to the i^{th} node, $T_{iCharge}$ is the time required to charge the i^{th} ECD, $T^*_{N^{th}Charge}$ is the time required to charge the Nth ECD, $T_{iTakeoff}$ is the time required to takeoff from the ground/base station, $T_{iDistance}$ is the time required to travel the distance between (i-1) to i^{th} node, T_{iLand} is the time required for landing, $SoC_{Maximum}$ is the maximum charge percentage of the battery, $T_{NCurrent}$ is the current charge percentage of the battery, and CC is the charging constant. This article concentrates on charging these ECDs using the shortest path and the most energy-saving algorithm for a drone to charge multiple ECDs at one flight mission.

III. PRIORITIZED DIJKSTRA'S ALGORITHM

This section is divided into two sections: ECD prioritizing algorithm and prioritized Dijkstra's algorithm. In the prioritizing algorithm, data from each node is gathered and a priority queue is formed, determining which ECDs need to be charged immediately. In the prioritized Dijkstra's algorithm, the said priority queue determines the shortest path and the energy consumption per drone's flight cycle. This allows a maximum number of ECDs to be charged with a minimum number of flight missions, effectively using the drone's flight time.

A. ECD PRIORITIZING ALGORITHM

In the ECD prioritizing algorithm, the known variables such as the last known battery percentage, the last time the ECD was charged, the number of ECDs to be charged, and the distance between the ECDs, are considered. These values are then arranged into the priority array (P_i). As seen in *Algorithm 1*, the ECDs, whose battery charge percentage is less than a minimum value will be added to the *P** array. Based on the above-mentioned parameters, 1-7 of *Algorithm 1*, a priority is assigned to individual ECDs.

From 8-19 of *Algorithm 1*, the ECDs are aligned in decreasing order of priority. Now, the algorithm prepared the ECDs that needs to be charged. Furthermore, to maximize the number of ECDs to be charged, the *Algorithm 2* comes into action.

Algorithm 1: Setting up the priority of ECDs based on the known variables

Input:
C_{Prev} : Last known battery charge percentage (Known variable)
H : Number of hours from previous charge (Known variable)
L_{Cycle} : Percentage decrease in charge per cycle of operation (Known variable)
D_N : Distance of ECD from the base station (Known variable)
N : Number of ECDs to be charged (Known variable)
Output: Priority of each ECD, $P^* = (P_1, P_2, P_3, P_4, \ldots. P_N)$
Start
Loop:
1. Find number of ECDs active and that needs to be charged
2. Assign, $P_1, P_2, P_3, P_4, \ldots\ldots P_N = 0$.
   Initializing priority of each ECD to be the same
3. Initialize, $i = 1$
4. **For** $P_i \leq P_N$
5. Compute: $P_i = C_{Prev} - (H \times L_{Cycle}) \times 100 + D_{Base}$
6. Increment $i = i + 1$, till i < = N
7. **End for**
8. Sort P* array in the decreasing order or priority
9. Initialize $i = 0, j = i+1$, temporary variable $temp = 0$
10. **For** i < length of (P^*)
11. **For** j < length of (P^*)
12. if($P^*[i] < P^*[j]$)
13. temp = $P^*[i]$
14. $P^*[i] = P^*[j]$
15. $P^*[j]$ = temp
16. increment $j = j + 1$, till j < = length of (P^*)
17. **End For**
18. increment $i = i + 1$, till i < = length of (P^*)
19. **End For**
End Loop

B. PRIORITIZED DIJKSTRA'S ALGORITHM

Using the logic of the Dijkstra's algorithm, the ECDs in the *P** array are aligned such that a shortest path with the least energy consumption and maximized number of ECDs to be charged is predicted. As seen in *Algorithm 2*, initially, the number of ECDs that can be charged is selected from the *P** array. Suppose, the drone has the energy equivalent to charge the first five ECDs during its current mission, the first five ECDs parameters are introduced into the path graph (G). This allows the *Algorithm 2* to decide a shortest path connecting the ECDs with the highest priority. The term prioritized in the manuscript refers to the arrangement of the ECDs in the G. In he original algorithm, all the nodes are given equal priority, whereas in the proposed version of Dijkstra's algorithm, based on the charge requirement of the ECDs, the priority of the ECDs changes, thus, the *Algorithm 2* is forced to select the ECD with the highest priority as its first node, and similarly selecting the next nodes. This ensures that the drone can charge multiple ECDs in one mission requiring immediate attention.

Algorithm 2: Prioritized Dijkstra's algorithm for shortest path generation between prioritized ECDs

Input:
Prioritized *P** Array of ECDs that needs to be charged= $(P_1, P_2, P_3, \ldots P_N)$
G = Path graph of P* nodes containing information such as distance from base station and adjacent node.
S = Base station location
Initially, select the ECDs that needs to immediately charged from the *P** array whose total energy requirement is less that the energy available with the drone

Output: A shortest path covering all the assigned ECDs
Start
Loop:

```
Dijkstra_shortest_path(G, S):
  Initializing for each vertex V in G:
  distance[v] := infinity   //distance between all the vertices
  previous[v] := undefined
  distance[S] := 0          //distance to base is allotted as '0'
  Q := set consisting of all nodes in Graph
  while Q != NULL set:
    U := node in Q with least distance[ ]
      POP U from Q
    for each neighbor V of U:
     new_dist := distance[U] + distance_between(U, V)
     if new_dist < distance[V]
       distance[V] := new_dist
       previous[V] := U
     return previous[ ]      //Return the path graph
Q becomes empty and awaits new nodes to be added
```

End Loop

IV. RESULTS AND DISCUSSIONS

The results and discussions section is divided into three sub-sections: Results during the wireless charging of the drone by the base charging station results during the drone to ECD charging and case studies of the proposed system.

A. DRONE CHARGING

The 24 V, 3 A constant PV power output is fed to the inverter circuit of the base charging station, which gives a high-frequency AC signal to the Tx coil. When the drone is ready to be charged, it switches to Mode 1 (Fig. 7), and the S_1, S_2, S_3 and S_4 switches are triggered at 84 kHz frequency. As the concept of WPT works on the principle of loosely coupled transformer with air core, when the Rx coil of the drone links with the induced EMF of the Tx coil (Fig. 9), an alternating current is produced in the drone's Rx coil. The alternating waveform's magnitude varies with the distance between the Tx-Rx coils. As shown in Fig. 10, with a larger gap between the Tx-Rx coils, less useful power is able to transfer. The power transfer capacity can be further increased with the addition of ferrite bars; however, due to the weight constraint, the ferrites are added only to the Tx coils. The proposed system's maximum power transfer efficiency occurs at 0-5 mm displacement between Tx-Rx coils. It is observed that at 10 mm displacement, 72 W of power can be received in the Rx coil with a total power transfer efficiency

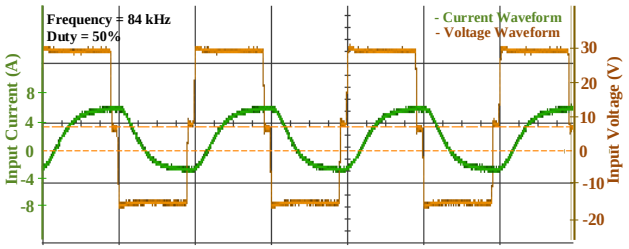

FIGURE 9. Input voltage-current waveform of the base charging station during constant voltage charging

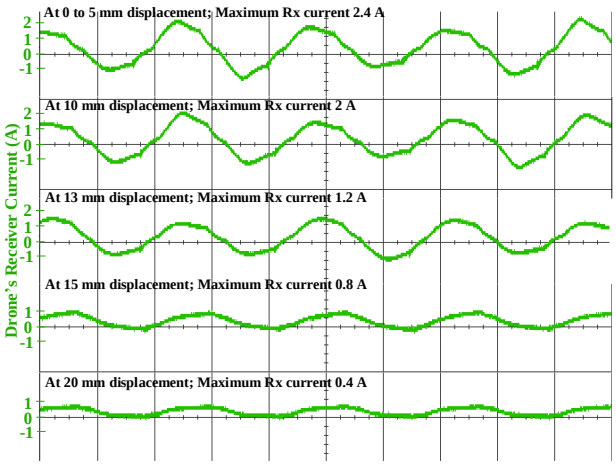

FIGURE 10. Output current waveform in the drone WPT circuit fed to the charge controller at constant-voltage mode, before rectification.

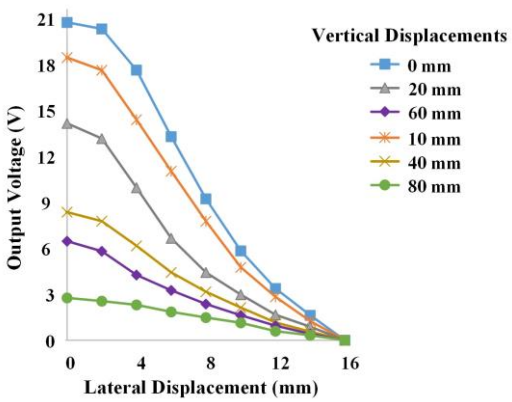

FIGURE 11. DC Output at various intervals of vertical and lateral displacement at the receiver side of the drone charging circuit.

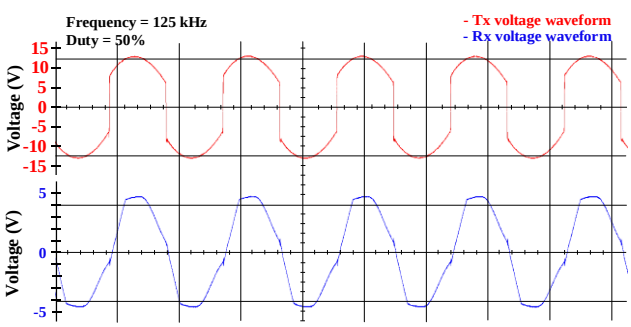

FIGURE 12. Output Waveform across ECD's battery charging circuit during Drone-to-ECD charging

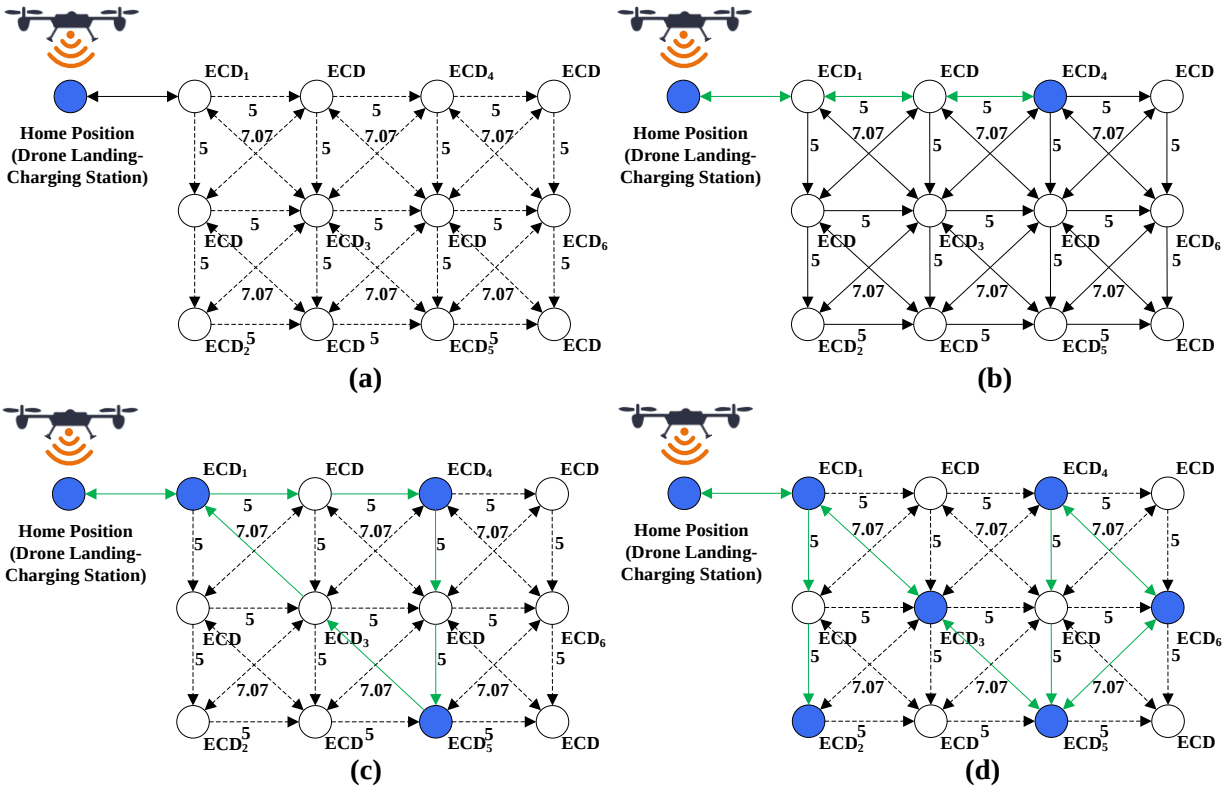

FIGURE 13. ECD Charging Case Studies (a) ECD placement in a field (b) Case 1, when one ECD is charged (c) Case 2, when three ECDs are needed to be charged (d) Case 3, when multiple ECDs are needed to be charged

of 91.3%. Due to Mode 1 operation, a rectified power signal is fed to the charge controller. The DC output across the receiver side in the drone charging circuit has been portrayed in Fig. 11.

B. DRONE TO ECD CHARGING

When the drone reaches the designated ECD, the charge controller shifts the operation to Mode 2, in which, the Rx coil of the drone now acts as Tx coil and the switches S'_1, S'_2, S'_3 and S'_4 pulsate at 125 kHz to form high-frequency AC waveform, shown in Fig. 12. The choice of higher-frequency is due to the smaller size of the Rx coil and the electrical components used in the ECD. Due to the ECD's smaller capacity, the Tx coil's power transfer is limited to 12 V and 0.5A. At the Rx side, 5 V and 1 A power is received at a constant distance of up to 10 mm. Due to the lower capacity of the ECD, transferring a higher power rating in WPT damages the ECDs internal components; thus, the power transfer is limited to 5 W. However, the WPT is efficient even when the device is buried 10 mm underground. Further studies are required to precisely adjust the drone's Tx coil on top of the ECD for maximized WPT.

C. CASE STUDIES

For ease of understanding of the working of the proposed system, three case studies are presented (Fig. 13). In the first case study, a single ECD is required to be charged. In the second case study, three ECDs are required to be charged and multiple ECDs are charge in case 3. The estimated energy consumption and time requirement models for the mission are presented in detail.

1) Case study 1

In this case, the available energy with the drone can charge one ECD, as shown in Fig. 13 (b). The ECD to be charged is running at 40% capacity, i.e., 40% of 600 mAh ≈240 mAh. It needs to be charged to 600 mAh; thus, the difference is 360 mAh. As per the battery's specifications, it can discharge at a 25 C rate, i.e., 25×600 mAh = 15A of discharging current. However, this is only possible for a short burst of time and it is not recommended, as it will damage the battery and the other electronic circuit. For safer operation, the charging rate should be preferred below 5C. As the proposed ECDs maximum handling capacity is 1.2 A, a 2C charging rate is preferred. As per the general rule, 1 C charging requires 1 hour of charging time, irrespective of its capacity. At the 2 C charging rate, the charging time reduces to 30 minutes. Short pulsating burst currents are introduced to further reduce the charging time. Thus, effectively reducing the charging time to half, i.e., a 600 mAh battery with 360 mAh charge required at a 1~2 C charging rate requires only 15 minutes of charging time. Thus, based on Eq. (15), the total time to charge ECD*$_3$ is the sum of time required to travel to ECD*$_3$, 15 minutes and the drone's travel time.

2) Case study 2

Considering the situation shown in Fig. 13 (c), three ECDs (ECD^*_1, ECD^*_3, and ECD^*_4) are to be charged. Considering ECD^*_1 is at 40% capacity, ECD^*_3 at 50% capacity, and ECD^*_4 at 60% capacity. As the number of ECDs exceeds 1, *Algorithm 1* and *Algorithm 2* come into action. *Algorithm 1* receives the ECDs data, computes the priority and stores it in the *P** array. The second half of the *Algorithm 1* arranges the ECDs into descending order of priority. The energy of the drone and the required energy to charge ECD are calculated. Suppose the energy level is sufficient to charge only ECD^*_1 and ECD^*_3. The drone has to make two trips, i.e., in trip 1, ECD^*_1 and ECD^*_3 will be charged and in trip 2, ECD^*_4 will be charged. To calculate the total time required to charge the ECDs will be determined by Eq. (15). During trip 1, the time required to charge the ECD^*_1 is the same as in case 1; thus, ECD^*_1 will charge in 15 minutes. In addition, ECD^*_3 is at 50% capacity; thus, the time required to charge ECD^*_3 is 20 minutes. Thus, the time required to charge the two ECDs is 35 minutes and considering the travel time from the base station to ECD^*_1 and ECD^*_1 to ECD^*_3, approximately 40~45 minutes is consumed. After its return to the base station, the drone goes into charging mode till the minimum requirement for trip 2. Similar to case 1, the process repeats for ECD^*_4.

3) Case study 3

Consider a special case shown in Fig. 13 (d) where six ECDs need to be charged and each ECD is ten units apart (ECD_3 at 7.07 units from ECD_1, ECD_2, ECD_4, and ECD_5) from each other. Let's assume it takes 10 seconds to travel ten units, takeoff/landing takes 10 seconds each and 30 seconds for the drone to recharge back. Then, when charging only one ECD, there is not much difference. However, when charging two ECDs (ECD_1 and ECD_2), in the case without the algorithm, the drone has to travel twice to the base station for recharging. Conversely, the drone with the algorithm would travel only once and charge both ECDs. Thus, the with algorithm uses 3.3% less time than the without algorithm model.

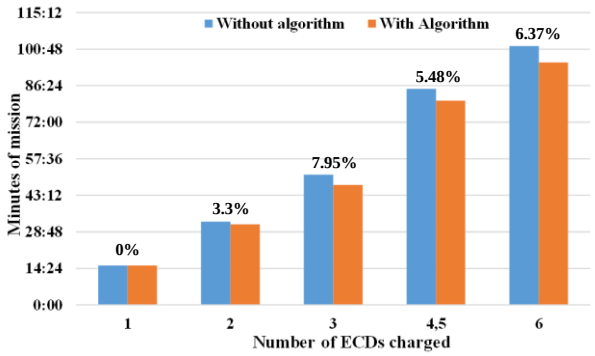

FIGURE 14. Case 3, charging multiple ECDs comparing with and without the proposed algorithm, numerical estimate analysis

D. DISCUSSION

Similarly, when charging three ECDs, a three-time flight mission to the base station and a single flight mission covering all the ECDs saves approximately 8% of the time. An estimated time saved bar graph is shown in Fig. 14. Considering that in the case of the proposed algorithm, the drone has to recharge after every three ECDs, a small dip in time saved is observed. This can be eliminated by using a bigger battery capacity to charge more ECDs in a single flight mission. A brief comparison of the proposed system vs. the existing systems is presented in Fig. 15.

The proposed system is useful when working with large agricultural sensors needing an autonomous charging facility. Furthermore, this algorithm ensures that all the ECDs are always fully charged using the autonomous bidirectional wireless charging drone. In the future scope, the system will be further analyzed with energy determination and prediction at each device. This would allow precise calculation and determination of path planning and energy management.

E. APPLICATIONS

Wireless charging drones have immense potential in shaping smart cities. They can be utilized for infrastructure inspection, emergency response, environmental monitoring,

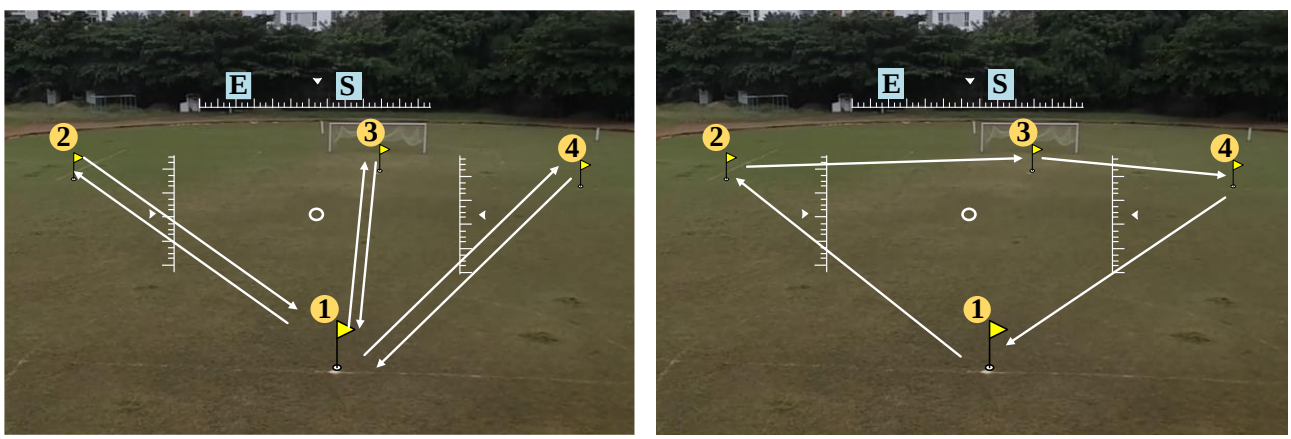

(a) (b)

FIGURE 15. Comparing conventional way of charging ECD with the prioritized Dijkstra's algorithm (a) Conventional charging (b) Proposed Dijkstra's prioritized model of charging with energy density

efficient delivery, urban surveillance, urban agriculture, and traffic governance. By harnessing the capabilities of these drones, smart cities can achieve enhanced efficiency, improved safety, better resource management, and sustainable development. With their versatility and flexibility, wireless charging drones offer a valuable solution to address a wide range of challenges and drive the advancement of smart city infrastructure and services.

F. Limitations

Wireless charging for drones and ECD devices offers many advantages, but it also comes with several challenges and problems. The significant challenges are:

1. The efficiency of wireless charging decreases with distance and misalignment between the charging coils. Achieving optimal alignment and close proximity between charging pads is challenging, leading to energy losses.
2. Wireless charging is generally slower compared to wired charging methods. For drones needing quick turnarounds between flights, this can be a limitation.
3. Wireless charging systems can interfere with other electronic devices or communication systems operating in the same frequency range.
4. Wireless charging systems generate heat, which can reduce the overall efficiency and, in some cases, damage batteries or electronic components if not properly managed.
5. Charging pads need to be strategically placed for coverage. Drones and ECDs outside the charging range cannot benefit from wireless charging, requiring careful infrastructure planning.
6. There are safety concerns regarding exposure to electromagnetic fields generated during wireless charging to animals and birds.

Addressing these challenges requires continuous advancements in wireless charging technology, improved standardization, and careful consideration of safety, efficiency, and environmental impact in the design and implementation.

V. CONCLUSION

In this paper, an algorithm to charge multiple agriculture sensors using a prioritized Dijkstra's algorithm has been proposed. Furthermore, a wireless charging drone landing station, a bidirectional charging drone and a wireless charging ECD for monitoring soil parameters have been developed. These devices aid in autonomous charging without the need for any medium of physical contact. The proposed wireless charging system transfer 72 W of power efficiently at 91.3%, up to a displacement of 5 mm. The designed ECD's battery lasts up to 30 days on a single charge. The prioritized Dijkstra's charges the ECDs in immediate need by utilizing a minimum number of flight missions and maximizing the energy usage efficiency of the drone's battery.

The salient features of the manuscript are listed below:

- A wireless charging, soil parameter measuring sensor device called an ECD has been developed. A bidirectional charging drone and its charging-discharging circuit has been modelled.
- The ECD is a miniature device, which requires frequent charging. The utilization of the sensor per hour determines the battery life of the sensor. When used 10 seconds per minute, the battery lasts 13 hours.
- To increase the battery life, the sensor can be operated 10 seconds per hour, which would give 30 days of battery backup.
- Since, these sensors are completely sealed and embedded in the ground, charging them via contact based method is difficult, thus wireless charging is proposed. To automate the charging of the ECDs, a bidirectional charging drone is deployed.
- The bidirectional charging drone is fed the data of the ECDs that needs to be charged and a prioritized path is planned for the drone to travel and charge each ECD.
- The charging characteristics of the ECD and multiple case studies comparing the path planning algorithm with and without a prioritizing algorithm have been illustrated in detail.

REFERENCES

[1] F. Veroustraete, "The rise of the drones in agriculture," *EC agriculture*, vol. 2, pp. 325-327, 2015.

[2] M. Aloqaily, O. Bouachir, I. Al Ridhawi, and A. Tzes, "An adaptive UAV positioning model for sustainable smart transportation," *Sustainable Cities and Society*, vol. 78, p. 103617, 2022.

[3] V. Puri, A. Nayyar, and L. Raja, "Agriculture drones: A modern breakthrough in precision agriculture," *Journal of Statistics and Management Systems*, vol. 20, pp. 507-518, 2017.

[4] N. Telagam, N. Kandasamy, and M. Arun Kumar, "Review on Smart Farming and Smart Agriculture for Society: Post-pandemic Era," in *Green Technological Innovation for Sustainable Smart Societies*, ed: Springer, 2021, pp. 233-256.

[5] M. ElSayed, A. Foda, and M. Mohamed, "Autonomous drone charging station planning through solar energy harnessing for zero-emission operations," *Sustainable Cities and Society*, vol. 86, p. 104122, 2022.

[6] R. Lyu, J. Pang, X. Tian, W. Zhao, and J. Zhang, "How to optimize the 2D/3D urban thermal environment: Insights derived from UAV LiDAR/multispectral data and multi-source remote sensing data," *Sustainable Cities and Society*, vol. 88, p. 104287, 2023.

[7] S. Sadowski and P. Spachos, "Wireless technologies for smart agricultural monitoring using internet of things devices with energy harvesting capabilities," *Computers and Electronics in Agriculture*, vol. 172, p. 105338, 2020.

[8] H. Sharma, A. Haque, and Z. A. Jaffery, "Maximization of wireless sensor network lifetime using solar energy harvesting for smart agriculture monitoring," *Ad Hoc Networks*, vol. 94, p. 101966, 2019.

[9] D. W. Sambo, A. Forster, B. O. Yenke, I. Sarr, B. Gueye, and P. Dayang, "Wireless underground sensor networks path loss model for precision agriculture (WUSN-PLM)," *IEEE Sensors Journal*, vol. 20, pp. 5298-5313, 2020.

[10] D. Xue and W. Huang, "Smart agriculture wireless sensor routing protocol and node location algorithm based on Internet

of Things technology," *IEEE Sensors Journal*, vol. 21, pp. 24967-24973, 2020.

[11] P. K. Chittoor, B. Chokkalingam, and L. Mihet-Popa, "A Review on UAV Wireless Charging: Fundamentals, Applications, Charging Techniques and Standards," IEEE Access, vol. 9, pp. 69235–69266, 2021, doi: 10.1109/access.2021.3077041.

[12] J. Shao, J. Cheng, B. Xia, K. Yang, and H. Wei, "A novel service system for long-distance drone delivery using the "Ant Colony+ A*" algorithm," *IEEE Systems Journal*, vol. 15, pp. 3348-3359, 2020.

[13] R. Alyassi, M. Khonji, A. Karapetyan, S. C.-K. Chau, K. Elbassioni, and C.-M. Tseng, "Autonomous recharging and flight mission planning for battery-operated autonomous drones," *IEEE Transactions on Automation Science and Engineering*, 2022.

[14] Q. M. Ha, Y. Deville, Q. D. Pham, and M. H. Hà, "On the min-cost traveling salesman problem with drone," *Transportation Research Part C: Emerging Technologies*, vol. 86, pp. 597-621, 2018.

[15] S. Kim and I. Moon, "Traveling salesman problem with a drone station," *IEEE Transactions on Systems, Man, and Cybernetics: Systems*, vol. 49, pp. 42-52, 2018.

[16] P. Perazzo, F. B. Sorbelli, M. Conti, G. Dini, and C. M. Pinotti, "Drone path planning for secure positioning and secure position verification," *IEEE Transactions on Mobile Computing*, vol. 16, pp. 2478-2493, 2016.

[17] N. B. Rossello, R. F. Carpio, A. Gasparri, and E. Garone, "Information-driven path planning for UAV with limited autonomy in large-scale field monitoring," *IEEE Transactions on Automation Science and Engineering*, vol. 19, pp. 2450-2460, 2021.

[18] A. M. Jawad, H. M. Jawad, R. Nordin, S. K. Gharghan, N. F. Abdullah, and M. J. Abu-Alshaeer, "Wireless power transfer with magnetic resonator coupling and sleep/active strategy for a drone charging station in smart agriculture," *IEEE Access*, vol. 7, pp. 139839-139851, 2019.

[19] C. Su, F. Ye, L.-C. Wang, L. Wang, Y. Tian, and Z. Han, "UAV-assisted wireless charging for energy-constrained IoT devices using dynamic matching," *IEEE Internet of Things Journal*, vol. 7, pp. 4789-4800, 2020.

[20] L. Zhao, D. J. Thrimawithana, and U. K. Madawala, "Hybrid bidirectional wireless EV charging system tolerant to pad misalignment," *IEEE Transactions on Industrial Electronics*, vol. 64, pp. 7079-7086, 2017.

[21] M. Huang, Y. Lu, and R. P. Martins, "A reconfigurable bidirectional wireless power transceiver for battery-to-battery wireless charging," *IEEE Transactions on Power Electronics*, vol. 34, pp. 7745-7753, 2018.

[22] B. Vardani and N. R. Tummuru, "A single-stage bidirectional inductive power transfer system with closed-loop current control strategy," *IEEE Transactions on Transportation Electrification*, vol. 6, pp. 948-957, 2020.

[23] Z. Wang, Y. Shi, and T. Meng, "Study on novel bidirectional AC-DC converter circuit of the wireless charging for portable devices," *IEEE Access*, vol. 8, pp. 198091-198100, 2020.

[24] Y. Li, X. Ni, J. Liu, R. Wang, J. Ma, Y. Zhai, *et al.*, "Design and Optimization of Coupling Coils for Bidirectional Wireless Charging System of Unmanned Aerial Vehicle," *Electronics*, vol. 9, p. 1964, 2020.

[25] W. Han, K. Chau, C. Jiang, W. Liu, and W. Lam, "Design and analysis of quasi-omnidirectional dynamic wireless power transfer for fly-and-charge," *IEEE Transactions on Magnetics*, vol. 55, pp. 1-9, 2019.

[26] C. Cai, S. Wu, L. Jiang, Z. Zhang, and S. Yang, "A 500-W wireless charging system with lightweight pick-up for unmanned aerial vehicles," *IEEE Transactions on Power Electronics*, vol. 35, pp. 7721-7724, 2020.

[27] C. Song, H. Kim, Y. Kim, D. Kim, S. Jeong, Y. Cho, *et al.*, "EMI reduction methods in wireless power transfer system for drone electrical charger using tightly coupled three-phase resonant magnetic field," *IEEE Transactions on Industrial Electronics*, vol. 65, pp. 6839-6849, 2018.

[28] T. Campi, S. Cruciani, and M. Feliziani, "Wireless power transfer technology applied to an autonomous electric UAV with a small secondary coil," *Energies*, vol. 11, p. 352, 2018.

[29] Y. Yan, W. Shi, and X. Zhang, "Design of UAV wireless power transmission system based on coupling coil structure optimization," *EURASIP Journal on Wireless Communications and Networking*, vol. 2020, pp. 1-13, 2020.

[30] Y. Li, W. Sun, J. Liu, Y. Liu, X. Yang, Y. Li, *et al.*, "A new magnetic coupler with high rotational misalignment tolerance for unmanned aerial vehicles wireless charging," *IEEE Transactions on Power Electronics*, vol. 37, pp. 12986-12991, 2022.

[31] C. Rong, X. He, Y. Wu, Y. Qi, R. Wang, Y. Sun, *et al.*, "Optimization design of resonance coils with high misalignment tolerance for drone wireless charging based on genetic algorithm," *IEEE Transactions on Industry Applications*, 2022.

[32] P. K. Chittoor and C. Bharatiraja, "Wireless-Sensor Communication Based Wireless-Charging Coil Positioning System for UAVs With Maximum Power Point Tracking," IEEE Sensors Journal, vol. 22, no. 8, pp. 8175–8182, Apr. 2022, doi: 10.1109/jsen.2022.3156089.

[33] A. Mahesh, B. Chokkalingam, and L. Mihet-Popa, "Inductive Wireless Power Transfer Charging for Electric Vehicles–A Review," IEEE Access, vol. 9, pp. 137667–137713, 2021, doi: 10.1109/access.2021.3116678.

[34] P. K. Chittoor and B. Chokkalingam, "Wireless Electrification System for Photovoltaic Powered Autonomous Drone Charging," IEEE Transactions on Transportation Electrification, pp. 1–1, 2023, doi: 10.1109/tte.2023.3305022.

Prithvi Krishna Chittoor received the bachelor's degree in Electrical and Electronics Engineering from Sree Vidyanikethan Engineering College, Tirupati, India. In 2017, the Master of Technology degree in Robotics Engineering from SRM Institute of Science and Technology, Chennai, India 2019. He is currently pursuing a PhD degree in Wireless Charging Technologies for UAVs. His research interests mainly include automation, wireless charging and vision-based path navigation.

C. Bharatiraja (Senior Member, IEEE) received the Master of Engineering degree in power electronics and drives from the Government College of Technology, Anna University, Coimbatore, India, in 2006, the Ph.D. degree in electrical engineering from the SRM Institute of Science and Technology in 2015, the first postdoctoral degree from the Centre for Energy and Electric Power, Faculty of Engineering and the Built Environment, Tshwane University of Technology, South Africa, and the second postdoctoral degree from Northeastern University, Boston, MA, USA. He is currently working as a Professor with the SRM Institute of Science and Technology, Chennai, India. At present, he is handling funded projects from Indian Government (DST SERB) worth of Rs.15 Crores. He has authored more than 110 scientific papers.

RAJESH VERMA is an Associate Professor in the Department of Electrical Engineering at the King Khalid University, Abha, KSA. He has work experience of more than 20 years of teaching and administration at many reputed institutes in India including MNNIT-Prayagraj and many others. He also worked in the Telecom industry for 4 years at New delhi, India. He completed his B.E., M.E. and Ph.D. in Electronics and Communication Engineering from MNNIT, Prayagraj in 1994, 2001 and 2011 respectively. His research interests include computer network, MAC protocols, wireless and mobile communication systems, sensor networks, peer-to-peer networks, M-2-M Networks.

LUCIAN MIHET-POPA (Senior Member, IEEE) was born in 1969. He received the bachelor's degree in electrical engineering, the master's degree in electric drives and power electronics, and the Ph.D. and Habilitation degrees in electrical engineering from the Politehnica University of Timisoara, Romania, in 1999, 2000, 2002, and 2015, respectively. Since 2016, he has been working as a Full Professor in energy technology with the Østfold University College, Norway. From 1999 to 2016, he was with the Politehnica University of Timisoara. He has also worked as a Research Scientist with Danish Technical University from 2011 to 2014, and also with Aalborg University, Denmark, from 2000 to 2002. He held a postdoctoral position with Siegen University, Germany, in 2004. He is also the Head of the Research Lab ''Intelligent Control of Energy Conversion and Storage Systems'' and is one of the Coordinators of the Master's degree Program in ''Green Energy Technology'' with the Faculty of Engineering, Østfold University College. He has published more than 130 papers in national and international journals and conference proceedings, and ten books. He has served as a scientific and technical program committee member for many IEEE conferences. He has participated in more than 15 international grants/projects, such as FP7, EEA, and Horizon 2020. He has been awarded more than ten national research grants. His research interests include modeling, simulation, control, and testing of energy conversion systems, and distributed energy resources (DER) components and systems, including battery storage systems (BSS) [for electric vehicles and hybrid cars and vanadium redox batteries (VRB)] and energy efficiency in smart buildings and smart grids. He was invited to join the Energy and Automotive Committees by the President and the Honorary President of the Atomium European Institute, working in close cooperation with—under the umbrella—the EC and EU Parliament, and was also appointed as the Chairman of AI4People, Energy Section. Since 2017, he has been a Guest Editor of five special issues of Energies (MDPI), Applied Sciences, Majlesi Journal of Electrical Engineering, and Advances in Meteorology journals.